

# Examining the Constellation of Scatterometers and Radiometers for Diurnal and Sub-Diurnal Wind Vector Variability

F. Joseph Turk and Svetla Hristova-Veleva  
Jet Propulsion Laboratory, California Institute of Technology  
Pasadena, CA USA    jturk@jpl.nasa.gov



The constellation of satellite-based ocean surface wind and precipitation observations since 1999 consists of a diverse collection of both sun-synchronous and asynchronous orbiting satellite platforms, both wind vector-capable (RapidScat, QuikSCAT, SeaWinds, ASCAT, OceanSat2, WindSat, RapidScat) and speed-only radiometers (TMI, GMI, AMSR, AMSR-2, SSMIS). These data can be jointly examined for time-of-day variability over regions where the surface wind varies widely throughout the day, owing to various meteorological forcings, such as land/sea temperature differences near coasts, or possible variations associated with tropical convective precipitation. Early results of an analysis are described whereby multiple wind speed and wind vector products were jointly examined to investigate the diurnal (and semi-diurnal, in cases) ocean wind vector variability.

## Theory

The formulation follows the structure of Gille *et. al.* (2005) and later used by Tang *et. al.* (2014), by modeling the diurnal wind using an elliptical variability, with the addition of the speed-only radiometers, the sub-diurnal terms, the error variance, and the capability to examine each day over the 2003-current period (when at least two scatterometers were jointly operating). Assume we have  $n$  wind vector estimates from  $n$  wind vector-capable satellite passes, all of them during a given day over a given location. This number varies depending upon the time of year, location, and the satellites being considered. The daily and sub-daily  $u$  and  $v$  components can be expressed with an elliptical fit using a compact matrix formulation:

$$\begin{bmatrix} u_1 \\ v_1 \\ \vdots \\ u_n \\ v_n \end{bmatrix} = \begin{bmatrix} a_0 + a_1 \cos(2\pi t_1/24) + a_2 \sin(2\pi t_1/24) + a_3 \cos(4\pi t_1/24) + a_4 \sin(4\pi t_1/24) \\ b_0 + b_1 \cos(2\pi t_1/24) + b_2 \sin(2\pi t_1/24) + b_3 \cos(4\pi t_1/24) + b_4 \sin(4\pi t_1/24) \\ \vdots \\ a_0 + a_1 \cos(2\pi t_n/24) + a_2 \sin(2\pi t_n/24) + a_3 \cos(4\pi t_n/24) + a_4 \sin(4\pi t_n/24) \\ b_0 + b_1 \cos(2\pi t_n/24) + b_2 \sin(2\pi t_n/24) + b_3 \cos(4\pi t_n/24) + b_4 \sin(4\pi t_n/24) \end{bmatrix} \begin{matrix} \vec{x} = (a_0 \ a_1 \ a_2 \ a_3 \ a_4)^T \\ \vec{y} = (b_0 \ b_1 \ b_2 \ b_3 \ b_4)^T \end{matrix}$$

$$[A] = \begin{pmatrix} 1 & \cos(2\pi t_1/24) & \sin(2\pi t_1/24) & \cos(4\pi t_1/24) & \sin(4\pi t_1/24) \\ \vdots & \vdots & \vdots & \vdots & \vdots \\ 1 & \cos(2\pi t_n/24) & \sin(2\pi t_n/24) & \cos(4\pi t_n/24) & \sin(4\pi t_n/24) \end{pmatrix}$$

$$\hat{\vec{x}} = (A^T D_u^{-1} A)^{-1} A^T D_u^{-1} U$$

$$\hat{\vec{y}} = (A^T D_v^{-1} A)^{-1} A^T D_v^{-1} V$$

For the speed-only (w) radiometers, since the relation between w and the  $u$  and  $v$  components is non-linear, hypothetical vectors are created by varying the directions one degree at a time (e.g., for one radiometer):

$$u_{n+1} = w \cos(\theta) = a_0 + a_1 \cos(2\pi t_1/24) + a_2 \sin(2\pi t_1/24) + a_3 \cos(4\pi t_1/24) + a_4 \sin(4\pi t_1/24)$$

$$v_{n+1} = w \sin(\theta) = b_0 + b_1 \cos(2\pi t_1/24) + b_2 \sin(2\pi t_1/24) + b_3 \cos(4\pi t_1/24) + b_4 \sin(4\pi t_1/24)$$

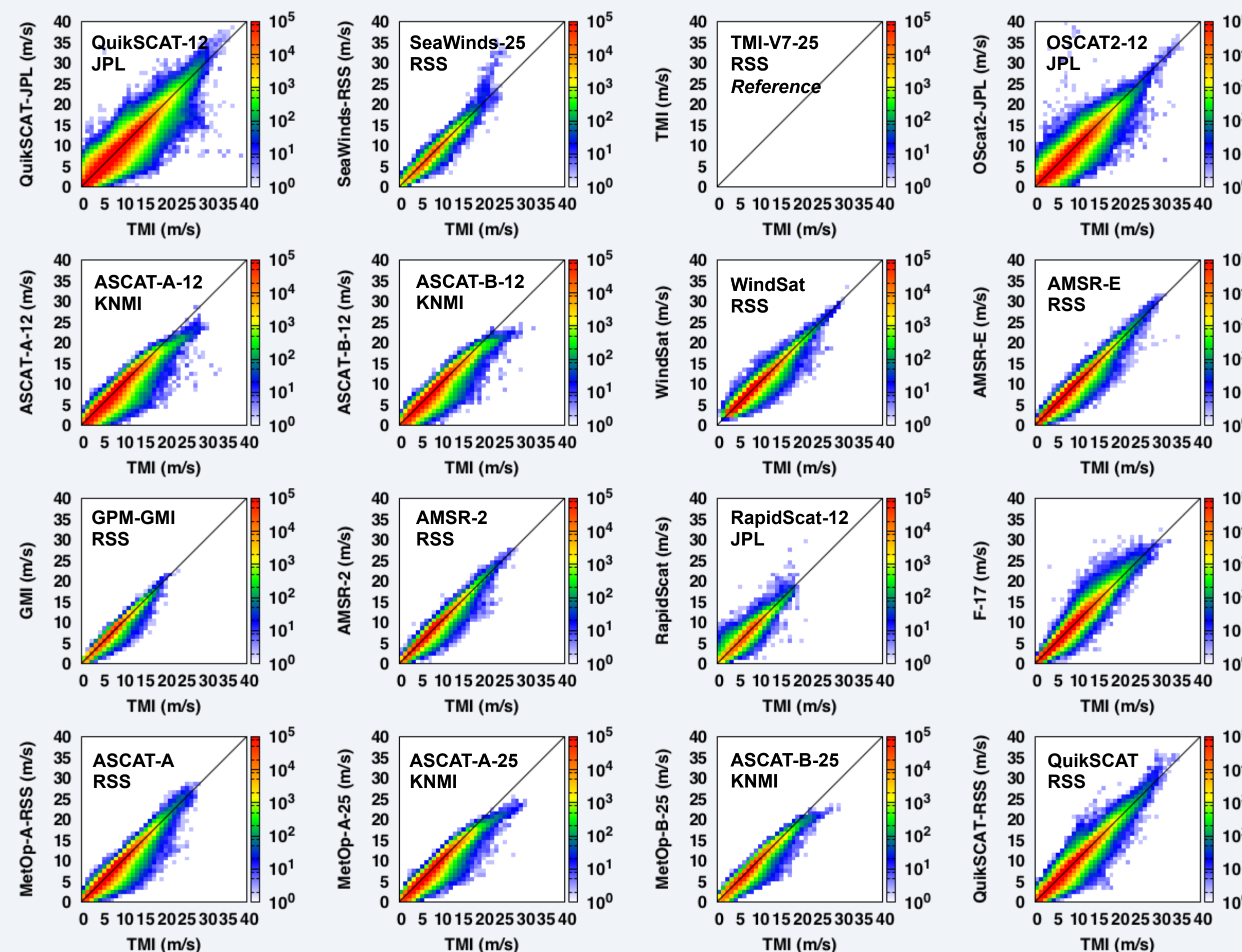
$$E(\theta) = \min \left( \sum_{i=1}^n (u_{n+1} - u_i)^2 + (v_{n+1} - v_i)^2 \right)$$

And locating the directions  $\theta$  that best agree with the observed vectors.

In either case, these expressions can be expressed in matrix form, where  $D_u$  and  $D_v$  are diagonal matrices with the variance of the  $u$  and  $v$  observations.

## Referencing to Common Sensor

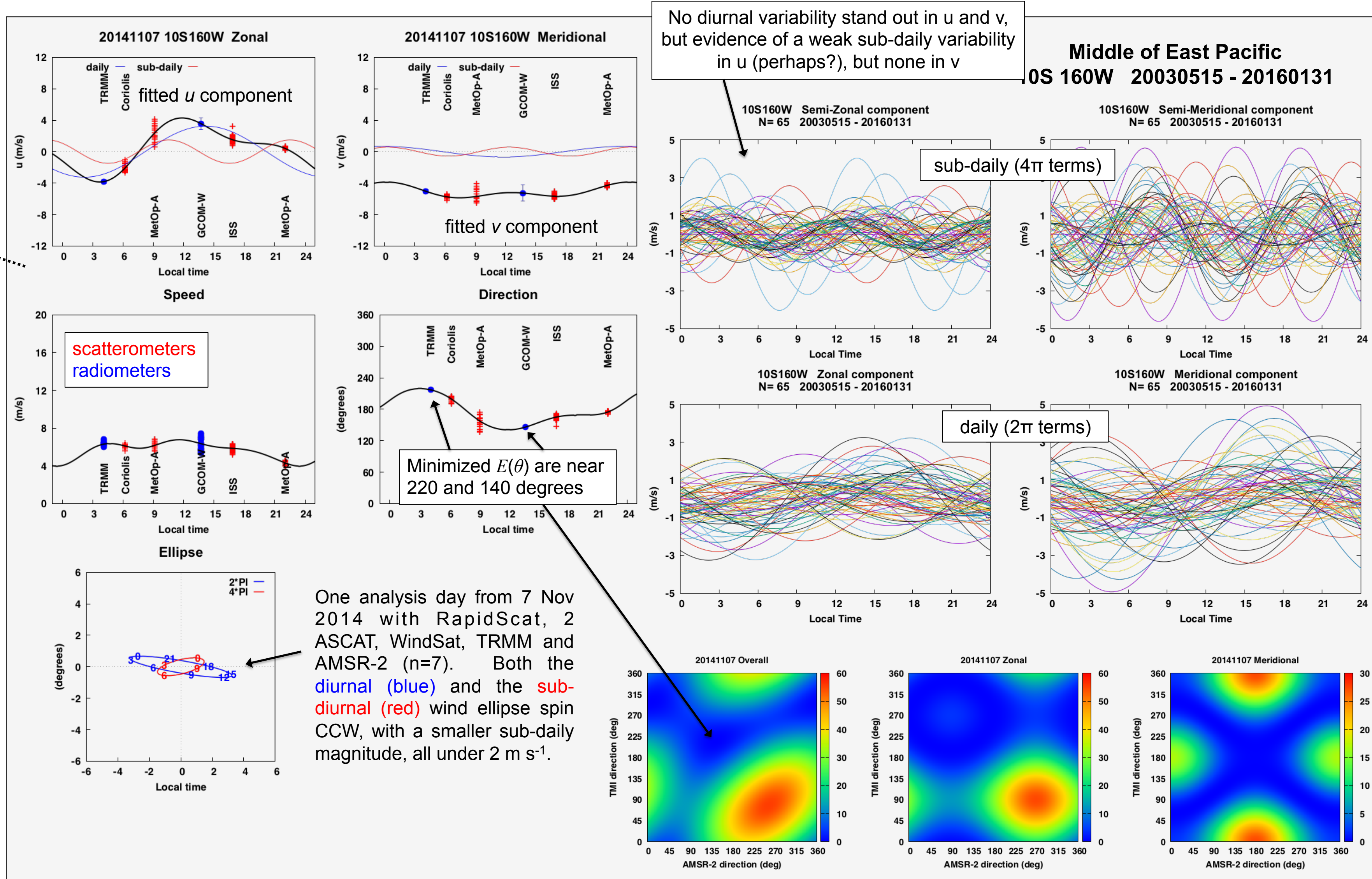
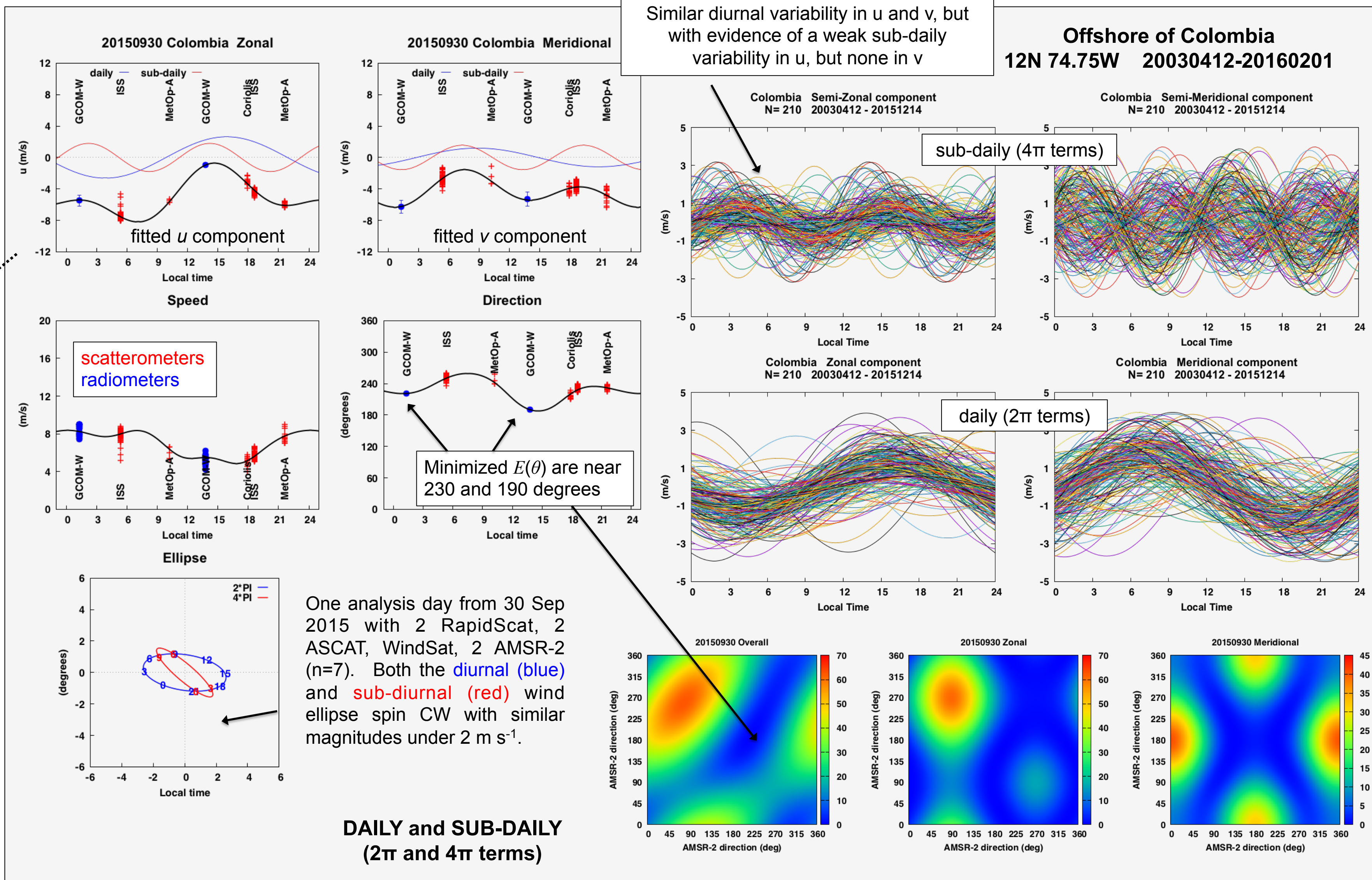
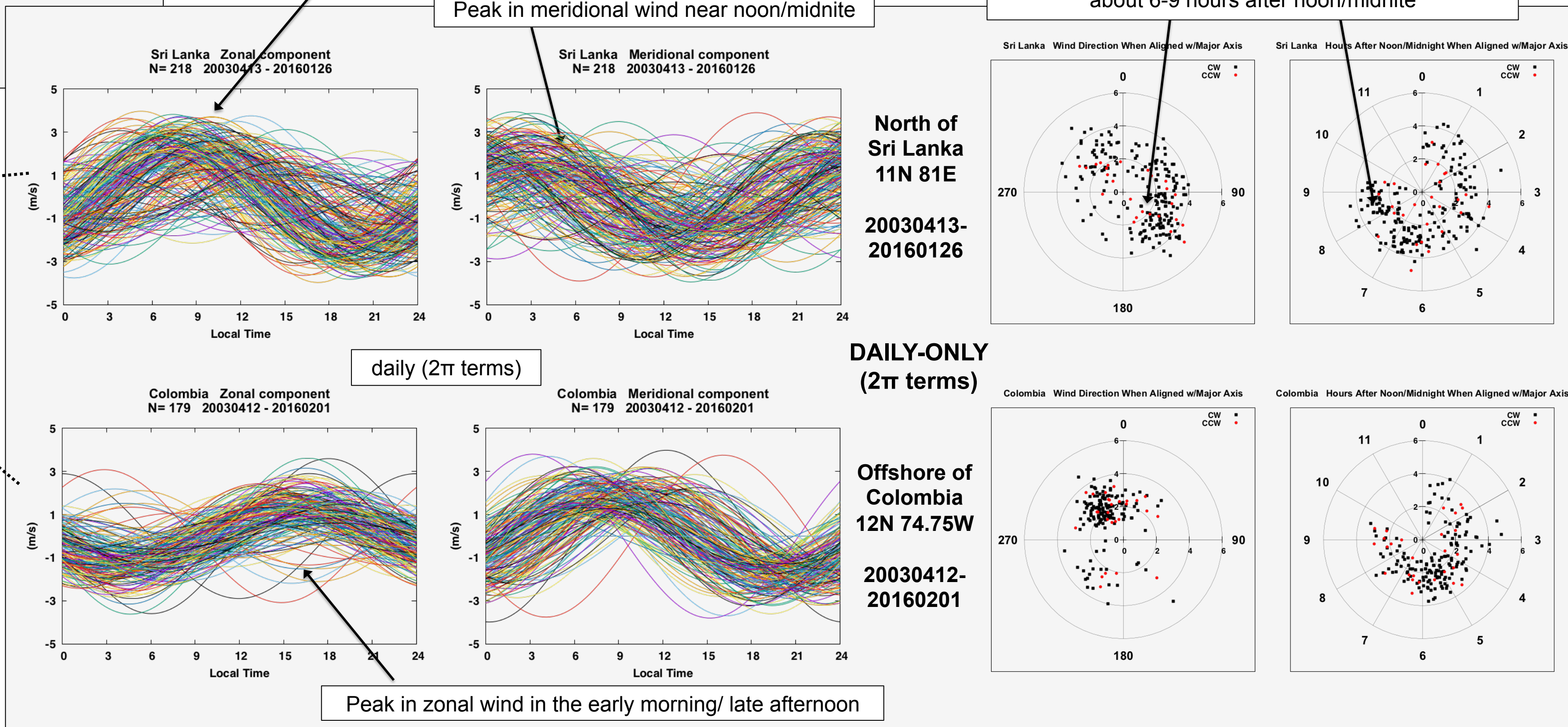
In this study, the asynchronous orbiting TRMM-TMI V7 0.25-degree wind speed products are used as a wind speed reference from 1999-2014, and GPM-GMI from April 2014-current, both produced by RSS (eight-month overlap period between TMI and GMI). Per-pixel coincidences within  $\pm 5$ -min between TMI (or GMI) and each of the 15 other different wind speed or wind vector (depending upon sensor type) datasets were collected over the Nov 1999-Mar 2016 period. Mean bias correction lookup tables were generated for each  $0.5 \text{ m s}^{-1}$  wind speed bin of the reference sensor. These were applied to adjust the speed each of the non-reference sensors, prior to any qualitative analysis.



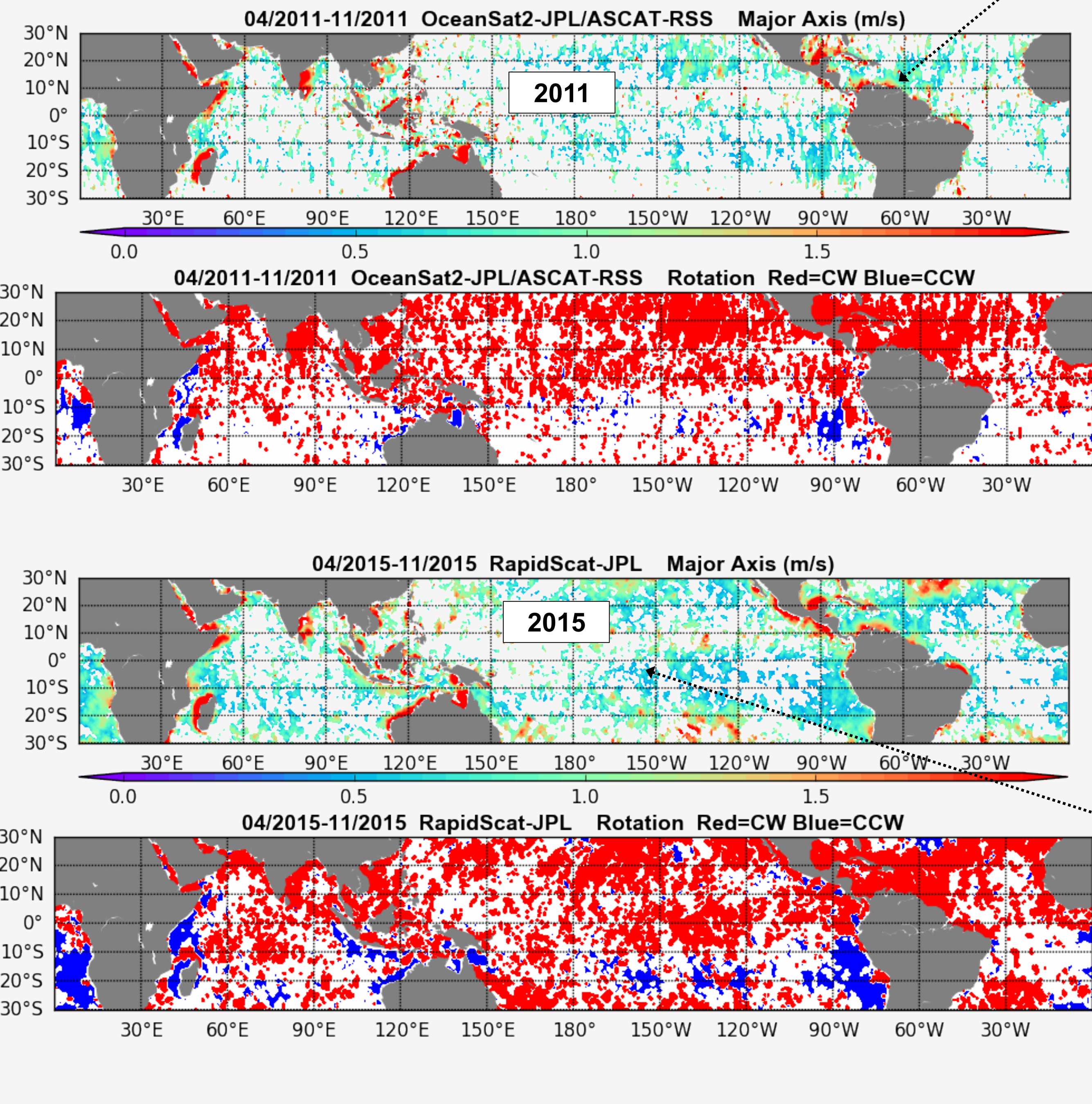
Peak in zonal wind in the morning/evening

Peak in meridional wind near noon/midnite

When the time is aligned with the major axis, winds are mostly SE or NW (180-deg ambiguity) and peak at about 6-9 hours after noon/midnite



The **top** panel shows the global map of the diurnal ellipse major axis ( $\text{m s}^{-1}$ ) and the direction of the ellipse rotation (red=CW, blue=CCW), derived from the April-November 2003 QuikSCAT-SeaWinds tandem mission ( $n=4 \text{ day}^{-1}$ ), which agrees closely with Fig. 1 of Gille *et. al.* (2005). This same analysis was repeated using the same months of 2011 with OceanSat-2-JPL and MetOp-A ASCAT-RSS (Version 2.1) (**middle**), and during same months during 2015 using only RapidScat-JPL (**bottom**). While there are slight differences in the areas of small diurnal magnitude over open ocean and in the southern hemisphere ellipse rotation direction, the patterns in general show good agreement. This suggests that RapidScat can be used for examining daily wind variability in places where the phenomena underlying the daily wind variability is sustained and captured over several RapidScat local time repeat cycles.



## All Acknowledgements

All radiometers, WindSat and ASCAT (V2) wind datasets were obtained from Remote Sensing Systems, Inc., (RSS) and are gratefully acknowledged. QuikSCAT, ASCAT, RapidScat and SeaWinds data were obtained from the Physical Oceanography Distributed Active Archive (PO.DAAC). The authors acknowledge support from the NASA OVW science team. This work was carried out at the Jet Propulsion Laboratory, California Institute of Technology, under a contract with NASA.

## References

Gille, S.T., *et. al.* (2005). Global observations of the land breeze. *Geophys. Res. Letters*, 32.  
Tang, W., *et. al.* (2014). Detection of diurnal cycle of ocean surface wind from space-based observations. *Int. J. Rem. Sens.*, 35, 5328-5341.